Monte Carlo study of vacancies in the bcc and hcp phases of ^{4}He

B. Chaudhuri, F. Pederiva, and G. V. Chester
Laboratory of Atomic and Solid State Physics, Cornell University, Ithaca, New York 14853
(Received 16 February 1999)

We use the shadow wave function formalism to determine the energy of formation of single and double vacancies in ^{4}He crystals at $T=0$ K. Data are presented for both the bcc and hcp phases. The activation energy for a single vacancy in bcc ^{4}He was found to be about 50% of that in hcp ^{4}He, which is approximately 15.6 K. By determining the occupation of the Voronoi regions around the crystal sites, we determine the location of vacancies in the crystal and studied the relaxation of the neighboring atoms. We also present data on the correlations between vacancies, and between vacancies and ^{3}He impurities. Following the position of the vacancy through successive configurations we observed the motion of the vacancy as seen in our Monte Carlo simulations. On the shorter Monte Carlo time scales, greater vacancy motion was observed in the bcc phase than in the hcp phase. [S0163-1829(99)07229-X]

I. INTRODUCTION

Vacancies in ^{4}He crystals have been intensively studied and there is now a wealth of experimental data available. Unfortunately these data have so far defied a consistent interpretation in terms of the phenomenological models that are available. These difficulties of interpretation have been reviewed[1–3] and a more recent discussion is given by Simmons.[4] It is believed that the vacancies in these crystals are highly mobile and should be thought of as delocalized in contrast with classical vacancies which diffuse relatively slowly through the crystal. Phenomenological models have been constructed[5,6] to describe these delocalized vacancies, or vacancy waves. However, these models lack the basic microscopic data which is necessary to make them reasonably quantitative. It is fair to say that there is no generally accepted microscopic picture of these vacancies and hence one's intuition is very limited.

There have been several experimental studies of vacancies in the bcc phase of solid ^{4}He.[7–9] Two of these studies[7,9] use NMR data on the relaxation of the nuclear spins of a dilute solution of ^{3}He in ^{4}He. These two studies are consistent with one another and strongly suggest that the energy of formation of a vacancy in the bcc phase is substantially lower than in the hexagonal crystal. The other striking feature of these experiments is that the motional narrowing of the resonance line of the ^{3}He nucleus is much larger in the bcc phase than in the hcp phase. This narrowing is attributed to motion induced by the vacancies and leads to the suggestion that the vacancies are more mobile in the bcc phase.

The x-ray studies of vacancies[8] in these two crystals disagree markedly with the results of the NMR studies. The x-ray data lead to the conclusion that the energy of formation is very similar for both crystals at the same density. In particular they find a very low activation energy in the hcp phase which leads to a large contribution to the specific heat,[1–3] which does not appear in the experimental data. There is a third NMR study[10] of dilute solutions of ^{3}He in solid ^{4}He which concludes that the activation energies of the bcc and hcp crystals are approximately the same. It is difficult for us to assess the quality of this work. However, it appears[9] that the quality of the crystals was not nearly as carefully controlled in these experiments when compared with those reported in Refs. 7 and 9. In particular it has been argued[9] that the dependence of the spin-spin relaxation time, T_2, on the concentration of ^{3}He strongly suggests that the crystals contain many dislocations where the ^{3}He was concentrated.

The purpose of this paper is to present the results we have obtained from Monte Carlo (MC) simulations of vacancies in the bcc and hcp phases of ^{4}He. Since the bcc phase only exists at finite temperatures we are simulating it as a metastable phase at absolute zero. A preliminary report of this work has been published.[11] In our current work we have computed the energies of formation, the way in which the neighbors relax around the vacancy, spatial correlations between vacancies and between a vacancy and a ^{3}He impurity. Finally, we have data on the mobility of the vacancies as seen in our Monte Carlo simulations. While our simulations have generated several interesting sets of data, only the energy of formation can, at present, be compared directly with experiment. Because the two NMR experiments[7,9] are consistent with one another and both provide data on the bcc and the hcp phases we have chosen these experiments with which to compare our data.

II. METHODS

A. Shadow wave functions

The shadow wave function[12,13] (SWF) for a system of N particles is defined by

$$\Psi(R)=\psi_R(R)\int \theta(R,S)\psi_S(S)dS. \tag{1}$$

Here, $\psi_R(R)$ and $\psi_S(S)$ are Jastrow wave functions defined for the set of atomic coordinates $R=\{\mathbf{r}_1\cdots\mathbf{r}_N\}$, and a set of auxiliary (shadow) variables, $S=\{\mathbf{s}_1\cdots\mathbf{s}_N\}$, respectively. The two types of variables are correlated by the Gaussian function $\theta(R,S)$. The functions in Eq. (1) are defined by the equations

TABLE I. The optimum values of the parameters in the wave function Eqs. (1) and (2). The parameters are defined in Eq. (3). The notation bcc ^{3}He (hcp ^{3}He) means that the C value for a single ^{3}He impurity in the host ^{4}He crystal has been optimized. All these parameter values are for the same density of $\rho = 0.028\,45\ \text{Å}^{-3}$.

Atom	b/σ	$C\sigma^2$	$\delta\,(\text{K}^{-1})$	α
bcc ^{4}He	1.080	5.20	0.11	0.860
bcc ^{3}He	1.080	3.95	0.11	0.860
hcp ^{4}He	1.080	5.48	0.11	0.872
hcp ^{3}He	1.080	4.51	0.11	0.872

$$\psi_R(R) = \exp\left[-\frac{1}{2}\sum_{i<j} u_{pp}(r_{ij})\right],$$

$$\psi_S(S) = \exp\left[-\sum_{i<j} u_{ss}(s_{ij})\right],$$

$$\theta(R,S) = \exp\left[-\sum_{i=1}^{N} u_{ps}(|\mathbf{r}_i - \mathbf{s}_i|)\right]. \tag{2}$$

The pseudopotentials $u_{\alpha\beta}$ are given by

$$u_{pp}(r) = (b/r)^5,$$

$$u_{ss}(s) = \delta v(\alpha r),$$

$$u_{ps}(r) = Cr^2, \tag{3}$$

where b, δ, α, and C are variational parameters, determined by minimizing the expectation of the Hamiltonian,

$$H = \frac{-\hbar^2}{2M_4}\sum_{i=1}^{N} \nabla_i^2 + \sum_{i<j} v(r_{ij}). \tag{4}$$

The interaction potential is the Aziz potential.[14] The pseudopotential u_{ss} is a scaled Aziz potential. The optimized values of the parameters are given in Table I.

The parameter C gives a measure of the kinetic energy of a particle. The smaller the value of C, the greater is the allowed deviation of the particle coordinate from the corresponding shadow coordinate, which implies a greater kinetic energy. For our calculations of the correlation between a ^{3}He impurity and a vacancy we changed the value of C for the ^{3}He atom and its value was determined by minimizing the energy of the system. The lighter mass of the ^{3}He impurity reduces C considerably. The ratio $C(3)/C(4)$ is approximately 0.8 for both the hcp and bcc crystals.

The SWF allows the atoms great freedom to organize themselves into the lowest energy state. This freedom is essential if we are to find a realistic description of a mobile vacancy in solid helium. The atoms must be free to move in such a way as to allow the vacancy to move. They must also be free to relax around the sites that the vacancy occupies during its motion. For these reasons the shadow wave functions provide an ideal tool with which to study these quantum vacancies. It is clear that the motion of the vacancy can only occur as a consequence of particles moving by at least one lattice spacing. This implies that we must describe the system by a wave function of the correct symmetry; our shadow wave function is fully symmetric in the coordinates of the helium atoms.

B. Simulation methods

Our simulation methods to determine the energy of vacancy formation are the same as those presented in the work by Pederiva *et al.*[12] The energy of formation of n_{vac} vacancies in a system of N particles and $N_l = N$ lattice sites with a density of $\rho = N/V$ is given by[12]

$$\Delta E_{\text{vac}} = [\epsilon(N - n_{\text{vac}}, \rho, N_l) - \epsilon(N, \rho, N_l)](N - n_{\text{vac}}), \tag{5}$$

where ϵ is the energy per particle.

Our simulations were primarily for the bcc and hcp crystals, but for purposes of comparison we also simulated the fcc crystal. A random walk in configuration space is generated using a modified Metropolis algorithm.[12] The length of each run, after equilibration, was 10^6 Monte Carlo steps, where one step is defined as a complete sweep of trial moves of all the particles and shadows. The activation energies of the vacancies were calculated using Eq. (5), by running simulations on a full lattice, and then on the same lattice with one atom removed. The density of the two systems were kept the same by altering the lattice parameter in the system with the vacancy. All our simulations were carried out at a density of $0.028\,45$ atoms Å^{-3}. This corresponds to a molar volume of 21.16, which is very close to the density at which the NMR experiments were carried out.

To study the motion of the vacancy and the correlations in which we are interested, the position of the vacancies had to be determined. This was done by associating every particle with a lattice site, by dividing the system into Voronoi regions (Wigner-Seitz cells in the bcc and fcc lattices) around the sites, and then determining whether a particle is inside or outside the Voronoi region of each site. An empty site is only labeled as a vacancy if each of the nearest-neighbor sites have only one particle. This rather complex definition is necessary because, in both the perfect and single vacancy crystal, particles can move so far from the lattice sites that they leave the original cell and occupy a next-nearest-neighbor cell. This appears to be a unique feature of the low-density quantum crystals. Thus in a perfect crystal we occasionally find an empty Voronoi region and a doubly occupied near-neighbor cell. We have previously labeled[12] this configuration a pseudointerstitial vacancy (PIV). This means that when we have a configuration of a crystal in which we have inserted a vacancy we will occasionally find two types of vacant cells. One type corresponds to a PIV, and for this vacancy, one near-neighbor cell is always doubly occupied. The other type is a genuine vacancy with no near-neighbor cell doubly occupied. In Sec. III E we discuss our data on PIV's in more detail. For the Wigner-Seitz cell of bcc crystal the next-nearest-neighbor is also a direct neighbor of a site, i.e., a site and its next-nearest neighbor share common boundaries. Hence, to define a vacancy in the bcc phase, the next-nearest neighbors were also required to have one particle each. The boundaries for the different Voronoi regions are defined as follows:

$$\text{bcc:} \pm x = a/2; \quad \pm y = a/2; \quad \pm z = a/2;$$

TABLE II. The activation energies for the three types of crystal. N is the number of lattice sites and $N-1$ is the number of particles when one vacancy is present. ΔE is the activation energy defined in Eq. (5). The two values for the bcc phase from Ref. 9 refer to two different models used to interpret the data.

Crystal	$N/N-1$	ΔE (Simulation)	ΔE (Expt.)
bcc	128/127	8.08±2.76	5.5±0.5[a]
	250/249	6.66±3.86	6.5±0.2[b]
	432/431	7.66±4.73	5.2±0.5[b]
hcp	180/179	15.63±3.85	15±1[a]
	448/447	15.55±4.63	14±3[b]
fcc	108/107	14.88±1.64	
	256/255	15.96±3.27	

[a]Reference 7.
[b]Reference 9.

$$\pm x \pm y \pm z = 3a/2,$$

$$\text{fcc:} (\pm x \pm y) = a/2; \quad (\pm y \pm z) = a/2; \quad (\pm z \pm x) = a/2,$$

$$\text{hcp:} \pm x = a/2; \quad \pm x \pm \sqrt{3} y = a; \quad \pm x + py \pm \sqrt{8} z = \sqrt{3} a;$$
$$-2py \pm \sqrt{8} z = \sqrt{3} a, \tag{6}$$

where a is the lattice spacing and $p=1$ for cells in an A plane, and $p=-1$ for cells in a B plane for the hcp crystal. Here A and B denote successive stacking planes for the hcp crystal. When determining the positions of the vacancies in each configuration, it was important to adjust the lattice for changes in the position of the center of mass of the system resulting from changes in the positions of the atoms, and of the vacancy. This was done by minimizing the average distance of the lattice sites from the position of the associated atoms.

III. RESULTS

A. Energies of vacancy formation

In Table II we show the activation energies for all three crystals. The activation energies for systems smaller than 128 particles for the bcc and 180 particles for the hcp crystal show significant size dependence. For these crystals, we therefore carried out calculations for systems of 432 and 448 particles, respectively. The results for the larger systems are in agreement with the results for systems of 128 and 180 particles, respectively, and we conclude that our data for these systems are reliable. The fcc crystal shows less size dependence and the activation energies agree for 108 and 256 particles. The size dependence for the bcc crystal arises, we believe, from the fact, discussed in Sec. III B, that there is appreciable relaxation in the neighborhood of vacancy; it extends out to the second neighbors. This means that the vacancy is in effect a large object and we, therefore, require a large system so that the images of the vacancy are sufficiently far apart. The same argument is unlikely to be valid for the hcp crystal, since the crystal distortion now only extends to the first neighbors. However, the noncubic arrangement of the atoms means that we again need a large number of particles before the images of the vacancy are sufficiently far apart. The lack of size dependence in the fcc lattice is, if the above arguments are accepted, therefore easily understood; there is distortion out to only the near neighbors and we have a close packed cubic crystal.

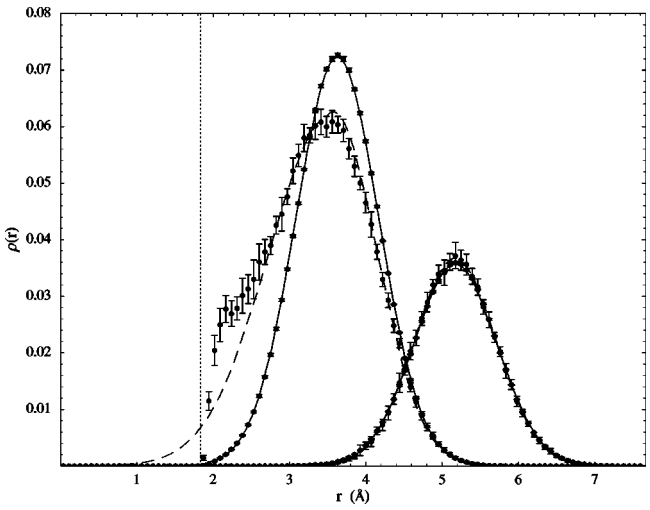

FIG. 1. The density distributions $\rho(r)$ of the near and the next-near neighbors of a filled site (——) and of a vacant site (− − −) for the hcp crystal. The dashed curve has been drawn as a guide to the eye. The density is normalized so that its integral over the three-dimensional volume is 1 for both nearest and next-nearest neighbor. There is an appreciable inward shift and broadening of the near-neighbor distribution and no change in the next-near-neighbor distribution. The dotted vertical line shows the position of the boundary of the central cell.

The errors in our activation energies are rather large. This is a consequence of the definition in Eq. (5), in which two energies very close in value are first subtracted and then multiplied by the number of particles. However, from our results it is clear that the activation energy for the bcc crystal is approximately one half of that in the hcp phase. In Table II we compare our activation energies with those found in the NMR experiments. The agreement is very satisfactory, however one would like to have smaller errors in both the simulation and experimental data. It is worth noting that the activation energies of both the closed-packed crystals are essentially the same. The activation energies in Table II are somewhat different from those we reported earlier.[11] First all our data are for crystals at a lower density and second for the hcp and bcc crystals we now have fully optimized wave functions. Our earlier data were based on unoptimized wave functions for these two crystals.

We have also simulated bcc and hcp crystals with two vacancies. The activation energies for these systems cannot be distinguished, within our errors, from twice the activation energy of a single vacancy. We will, however, see using a different approach, in Sec. III C, that it is likely that two vacancies are weakly bound.

B. Distribution of neighbors

The density distribution of the nearest neighbors and next-nearest neighbors around filled sites and vacancies are presented in Figs. 1 and 2. The origin of the x axis represents the center of either a filled or a vacant site. In both crystals

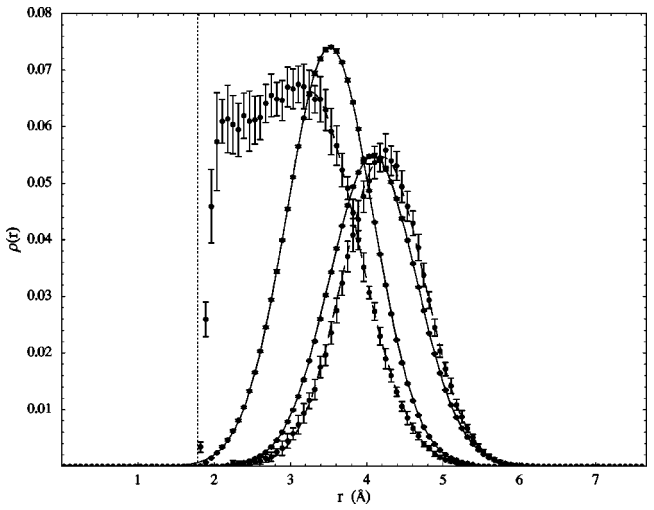

FIG. 2. The density distributions $\rho(r)$ of the near and the next-near neighbors of a filled (——) and a vacant site (— — —) for the bcc crystal. The dashed curve has been drawn as a guide to the eye. The density is normalized so that its integral over the three-dimensional volume is 1 for both near and next-nearest neighbor. There is a large shift inwards and broadening of the nearest-neighbor distribution, and the next-near neighbors show a definite outward shift. The dotted vertical line shows the position of the boundary of the central cell.

the distributions around the filled sites peak at the correct distances of the nearest and next-nearest neighbors. The integrated distributions yielded the correct number of nearest and next-nearest neighbors; both distributions are very accurately Gaussian. The curves shown have been normalized to one near and one next-nearest neighbor. The distribution of nearest neighbors around the vacancies in the hcp crystal is found to relax inwards, with the peak slightly shifted towards the vacancy. The next-nearest neighbors do not feel the presence of the vacancy, since no shift is observed in the corresponding distribution. As expected from the closed-packed nature of the fcc crystal, the distributions of the neighbors around vacancies in that crystal was found to be almost the same as that of the hcp crystal. In the bcc crystal the near neighbors of the vacancies undergo a much greater relaxation inwards compared to the hcp crystal. The next-nearest neighbors, however, move outwards by a significant amount, unlike those of the hcp crystal. It is plausible that the large inward relaxation of the near neighbors has forced the next-nearest neighbors to move out away from the vacancy.

We see a sharp cutoff in nearest-neighbor distribution of the vacancy at half the near-neighbor distance from the center of the vacancy. This arises from our definition of the vacancy, which constrains us to consider a site to be a vacancy only if the Voronoi cell is completely empty. This constraint causes the magnitude of the distribution, just beyond the cutoff, to be greater than the real value. This is because as the neighboring atoms of the vacancy relax towards it an atom can move into the Voronoi region of the vacancy. This should contribute to a tail of the distribution of the near neighbors of the vacancy. But according to our definition this site is no longer a vacancy, instead the site from which the particle moved is now the vacancy. Thus the values near the cutoff that would contribute to the tail, instead contribute to the distribution just before the cutoff.

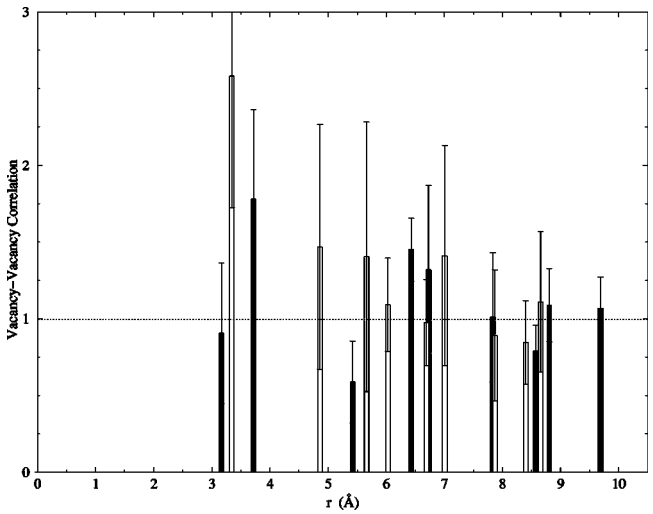

FIG. 3. The vacancy-vacancy correlations in the bcc and hcp crystals. The data shown in black are for the bcc crystal: that shown in white is for the hcp crystal. The correlation function has been normalized to unity at large distances. The data points all refer to sites in the crystal measured from one of the vacancies. The data points between 3 and 3.5 Å give the probability of finding the second vacancy as a near neighbor. The data between 3.5 and 4 Å give probability for the bcc lattice of finding the second vacancy as a next-near neighbor.

C. Vacancy-vacancy and impurity-vacancy correlations

Our data for the correlations between two vacancies and between a vacancy and ^{3}He impurity atom in a ^{4}He system are presented in Figs. 3 and 4.

The data for the correlation between two vacancies show that there is a strong correlation at the nearest-neighbor distance in the hcp crystal. The probability of finding two vacancies as near neighbors is approximately twice that of finding them at larger separations. At first sight a similar correlation is not present in the bcc crystal. However, as we have pointed out, due to the open nature of the bcc lattice, the next-nearest neighbors are also direct neighbors, i.e., the

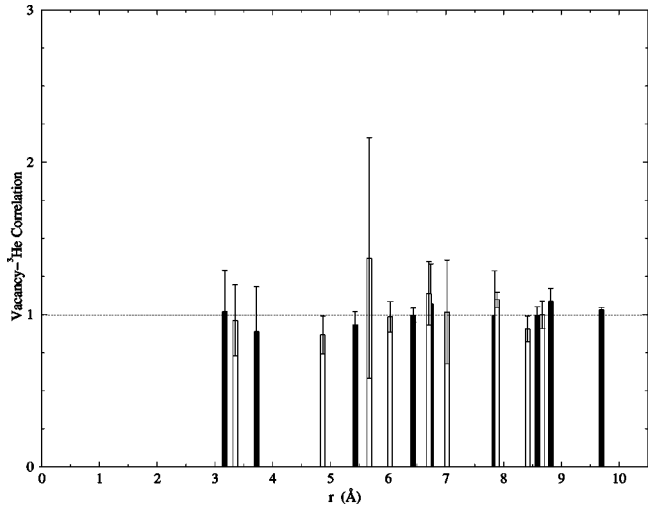

FIG. 4. The vacancy-^{3}He impurity correlations in the hcp (white) and bcc (black) crystal. The vacancy is at the origin and the data points refer to the position of the ^{3}He impurity. The system contained one vacancy and one ^{3}He impurity.

Wigner-Seitz cells of the next-nearest neighbors have common boundaries with the central cell. If we consider the nearest and next-nearest neighbors together for the bcc phase, then we do observe a strong correlation between the vacancies that are near neighbors, and the magnitude of the correlation is the same as for the hcp crystal.

A straightforward interpretation of the data in Fig. 4 shows no correlation between the ^{3}He impurity and vacancy. However, if we are willing to use the previous argument that the nearest and next-nearest neighbors in the bcc phase are similar in nature, in that they are both direct neighbors of the central cell, we can then combine the results of the two sets of neighbors. Doing so, we do observe a significant correlation between the ^{3}He impurity and the vacancy in this crystal.

D. Motion of vacancies

In our previous publication[12] we presented data that clearly showed that in a long Monte Carlo run a vacancy in solid ^{4}He moved rapidly throughout the crystal. We saw that every Wigner-Seitz cell of the fcc crystal had equal probability of being empty. The simulations we have made for our comparative study of vacancies in bcc and hcp ^{4}He provided new data on the ''motion'' of vacancies in these crystals. We must, however, emphasize that the motion we record is a consequence of our Monte Carlo moves as generated by our Metropolis algorithm and should be distinguished carefully from the real time motion of vacancies. Nevertheless, we hope that the behavior we observe in our MC runs will provide some physical insight into the behavior of these vacancies.

Since we were able to track the position of the vacancy throughout a run we used this information to calculate the mean-square distance the vacancy had moved as a function of the number of MC steps. The distance moved varied somewhat from run to run. We were, however, able to obtain accurate data by averaging across ten independent runs. We carried out this procedure for the bcc, hcp, and fcc lattices. Our raw data for the hcp and bcc crystals, together with the mean values, are shown in Fig. 5. The data for the fcc crystal were essentially the same as that for the hcp. In Fig. 6 we show the averages of that data plotted together for all three lattices. The long linear portions of the curves show very clearly that after about 20 MC accepted steps a simple MC diffusive motion sets in. Since the slopes of all three curves are nearly the same, the rate of diffusion through the lattice, as measured on a fairly long MC ''time'' scale, is the same in all three crystals. These curves imply that in about 4000 sweeps a vacancy will have traveled right across our simulation cell. Thus in a run of 10^6 sweeps the vacancy has visited every part of the crystal many times.

However, there is a marked difference in the curves for the short MC ''times;'' i.e., for less than about 20 MC accepted steps. It takes about 100 accepted steps for the hcp (or fcc) vacancy to travel one lattice spacing, and about 300 to travel two lattice spacings. However, for the bcc crystal the short distance motion takes place an order of magnitude more rapidly. One lattice spacing is reached in less than 10 steps, while two lattice spacings are reached after about 20 steps. Clearly the bcc vacancy is, under our MC algorithm,

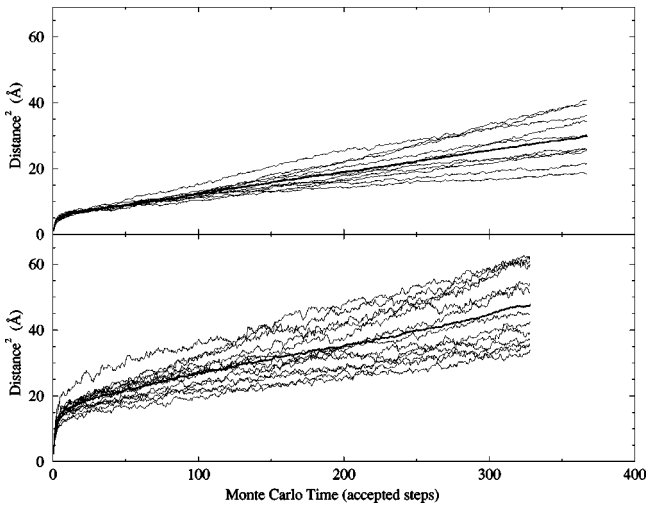

FIG. 5. Plots showing the mean-square displacement of a vacancy as a function of the number of MC moves in the system in hcp (top) and bcc (bottom) crystals. Individual runs generated data with a fairly wide spread of values for the distance traveled. We show in each graph ten of these runs (gray). The average over these runs is shown as a black curve.

making a large amount of local motion close to its original lattice site. In that sense it is much more delocalized than the hcp (or fcc) vacancy. There is probably a simple explanation for this. As we have already pointed out the second neighbors are close for the bcc lattice and share boundaries with the central cell. In other words the rapid local motion in the bcc crystal is a consequence of its much more open structure. It is, however, worth pointing out that the vacancy in the bcc crystal reaches three lattice spacings in about 200 accepted steps, which is considerably less than the 300 steps the hcp vacancy requires to reach two spacings. We speculate that

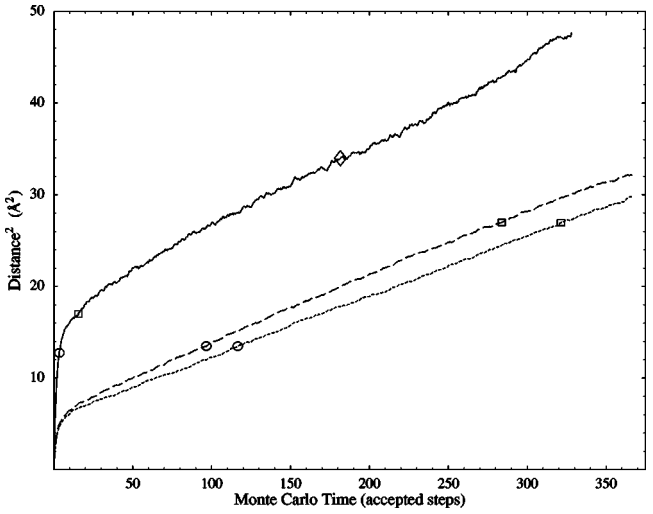

FIG. 6. The motion of vacancy in the three crystals. The mean-square distance traveled in the bcc (solid curve), hcp (dashed curve), and fcc (dotted curve) crystals as a function of the number of accepted MC steps. The circles on the curves show the number of steps required to reach the first-neighbor distance, the squares the number of steps to reach the second neighbor. The diamond shows the position of the third-nearest-neighbor for the bcc lattice.

the rapid MC motion of the bcc vacancy may provide an explanation for the much larger motional narrowing of the NMR signals observed in bcc crystals of dilute solutions of ^{3}He in solid ^{4}He.

E. Pseudointerstitial-vacancy pairs

In Sec. II we described the interstitial vacancy pairs (PIV) we find in our simulations. In our earlier paper we presented data on their occurrence in the fcc lattice. These vacancies arise when a particle makes a sufficiently large excursion from its lattice site that it enters one of the near-neighbor cells, and that cell becomes doubly occupied. The extra particle in the near-neighbor cell we call the interstitial. Very soon after this event takes place in the MC simulation the interstitial moves back into the vacant cell. This pseudovacancy is thus readily identified because one of the near-neighbor cells is always doubly occupied. We now present much more extensive and accurate data on the bcc, hcp, and fcc crystals. This data are at the single density 0.02845 Å^{-3}. We have studied the occurrence of these large amplitude fluctuations both in crystals with no vacancy present and also in crystals in which we have inserted a vacancy. The data for the PIV's came from several independent data sets of 6000 sweeps. We had 18 data sets for the hcp crystal with one vacancy and for the bcc crystal with one vacancy we had 13 sets. The corresponding numbers for the crystals without vacancies were 9 and 10, respectively. After some initial analysis it was clear that the data sets for the hcp crystals fell into two distinct classes; either they contained configurations with a fairly small numbers of PIV's, typically less than three and four which we consider as normal, or the configurations frequently contained between five and ten PIV's which we call abnormal. For the hcp crystal with one vacancy ten data sets showed normal behavior and eight were abnormal. The crystal with no vacancy was much more stable, only one out of nine data sets showed abnormal behavior. We, therefore, carried out separate analysis for these two kinds of data. We will present data that show fairly convincingly that when the simulation data show a relatively large numbers of PIV's then a whole lattice plane has shifted sideways by an appreciable amount. We present the abnormal PIV data at the end of our discussion.

In Fig. 7 we show the frequency of occurrence of PIV's for the hcp and bcc lattices for which we have not created a vacancy. The data for the fcc lattice are almost identical to that for the hcp. There are several interesting points. First for the hcp crystal we are as likely to find a configuration with a single PIV as we are to find none. Moreover, when we look at the frequencies of finding two, three, and four PIV's we realize that most configurations contain at least one PIV and often contain two or three. However, it is very rare to find more than five or six PIV pairs. The data for the bcc lattice, are very different. It is now nearly twice as probable to find one or two PIV's as it is to find none. Moreover, the distribution of PIV's is now broader and we have a significant number of configurations with six PIV's. We conclude that there are more large amplitude fluctuations in the bcc lattice than in the close-packed hcp lattice. The data for PIV's in these lattices when we have created a vacancy show very little change from the data for the full lattices. We conclude, as might be expected, that the presence of a single vacancy in a crystal of 180 or 250 particles does not affect the underlying large amplitude fluctuations. We can summarize the above analysis by saying that these large amplitude fluctuations are fairly common, we are more likely to find some PIV's in a configuration than none. In the case of the bcc crystal PIV's are even more frequent; local disorder is more common, we find that the mean number of PIV's for configuration for the hcp and fcc crystals is close to 1, while for the bcc crystal the number is twice as large. However, to compare these two numbers we must correct for the fact that they refer to different system sizes. When this correction is made we find that the bcc crystal has approximately 50% more PIV's than the hcp crystal. In each case the percentage of PIV's is of the order of 10^{-2} of the number of particles. While this is a small fraction, it is comparable to the concentration of vacancies at low temperatures.

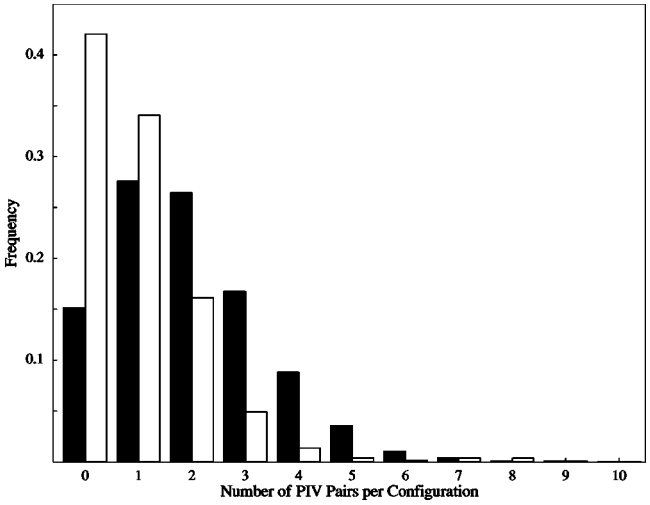

FIG. 7. The normalized frequency of occurrence of PIV pairs in the hcp (white) and bcc (black) crystal.

We now turn to the special case we mentioned earlier in which there are data sets for the hcp crystal that show relatively large numbers of PIV's. As we have mentioned the data for the crystal without a vacancy shows the behavior comparatively infrequently. However, the data for the crystal with one vacancy show that large numbers of PIV's occur in approximately half of the data sets. The frequency distribution of PIV's is shown in Fig. 8. We see a rather low frequency for small numbers of PIV's and a much larger frequency peaking at about seven and extending out to 11 or 12 PIV's. This distribution is thus completely different from our ''normal'' distribution. The mean number of PIV's in this distribution is approximately six. Clearly the creation of a single vacancy in 180 particle system frequently destabilizes the crystal and we find that one of the close packed planes has slipped into a different stacking position. We show this in Fig. 9. Because the new position is also an equilibrium position it is unlikely that the plane will readily slip back and this is confirmed by our data. It is possible that the position of the peak of the distribution of PIV's will depend on the size of the system being simulated. The larger the plane that slips the larger the mean number of PIV's that will be found. This implies that for larger systems the overall distribution will move to larger values. We could spend considerable

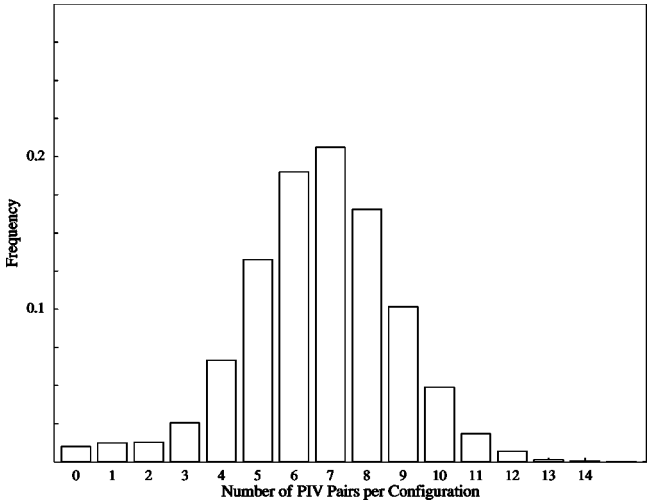

FIG. 8. The normalized frequency of occurrence of PIV pairs in the hcp crystal with one vacancy and when a lattice plane has slipped.

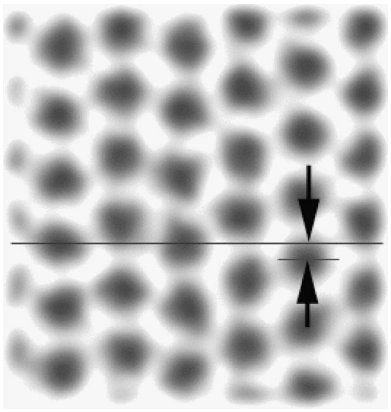

FIG. 9. This figure shows the position of a plane that has slipped. The plot is made by taking 400 configurations and for each configuration a point is plotted on the figure. Several hundred configurations are needed to show the region of space occupied by each particle. The original plot has been processed to provide a clearer picture of the positions of the particles. The lattice plane that is second from the right-hand edge has slipped by an amount shown by the two arrows.

time investigating this phenomenon. However, at this stage we need to be cautious because we do not know whether what we are seeing is an artifact of the wave function we are using. We plan to carry out runs on the hcp crystal with the best available[15] shadow wave function over a range of densities. The results of this investigation should help us understand whether the phenomenon is a real physical effect.

IV. DISCUSSION

The simulation data we have presented show a number of striking features. We summarize these and then make some comments on the NMR experiments in the bcc and hcp crystals.

Our data show that the properties of vacancies in the two closed-packed crystals, fcc and hcp, are, within our statistical errors, identical. There is one exception to this statement; a single vacancy appears to destabilize the hcp crystal and produce large numbers of PIV's. In contrast to the agreement of the data between the close-packed crystals the vacancies in the more open bcc crystal have very different properties; a much lower activation energy, much more distortion of the crystal around the vacancy, higher MC mobility and more local disorder as measured by the number of PIV's. One of the interesting experimental results is that the motional narrowing of the NMR signals from a dilute solution of ^{3}He in bcc ^{4}He is much less than that in the hcp crystal at the same density.[7,9] This is believed to be due to a faster motion of the ^{3}He atoms in the bcc phase. We have two pieces of evidence that support this conjecture. First, there is a fairly strong correlation of a ^{3}He impurity and a vacancy in the bcc crystal and second on a short-time scale the vacancies in the bcc crystal are much more mobile. Neither effect is present in the hcp crystal. We speculate that as the vacancy moves locally in the bcc crystal the ^{3}He impurity tends to move with it and this motion may be responsible for the greater motional narrowing.

There are a number of refinements that we plan to make in our calculations. First, we will use the fully optimized shadow wave functions that have recently become available.[15] Second, improved two-body potentials are also available.[16] The accuracy of our activation energies can be improved by using data from much longer runs. Two simulations appear to be interesting. First, we can modify our shadow wave function by incorporating into it a one-body factor to describe the binding of a ^{3}He impurity to a vacancy. Minimizing the parameters in the one-body function should lead to an estimate of the binding energy. Second, we plan to construct an excited-state wave function for a vacancy. This can readily be done within the shadow formalism[16] and should allow us to make contact with the phenomenological theory of vacancy waves.

ACKNOWLEDGMENTS

This work was carried out on the IBM SP-2 at the Cornell Theory Center which receives funding from Cornell University, New York State, the National Center for Research Resources at the National Institute of Health, the National Science Foundation, the Department of Defense Modernization Program, and members of the Corporate Partnership Program. F.P. was supported by the National Science Foundation under Grant No. ASC 9626329; Basudev Chaudhuri was supported in part by the Cornell Center for Materials Research.

[1] C. A. Burns and J. M. Goodkind, J. Low Temp. Phys. **93**, 15 (1993).
[2] B. A. Fraas, P. R. Granfors, and R. O. Simmons, Phys. Rev. B **39**, 124 (1989).
[3] N. E. Dyumin, N. V. Zuev, and V. N. Grigorev, Fiz. Nizk. Temp. **19**, 33 (1993) [Low Temp. Phys. **19**, 23 (1993)].
[4] R. O. Simmons, J. Phys. Chem. Solids **55**, 895 (1994).
[5] A. F. Andreev and I. M. Lifschitz, Zh. Eksp. Teor. Fiz. **56**,2057(1969) [Sov. Phys. JETP **29**, 1107 (1969)]; A. F. Andreev, *Progress in Low Temperature Physics* (North-Holland, Amsterdam, 1982), Vol. 8.
[6] R. A. Guyer, J. Low Temp. Phys. **8**, 427 (1972).
[7] D. S. Miyoshi, R. M. Cotts, M. Greenberg, and R. C. Richardson, Phys. Rev. A **2**, 870 (1970).
[8] P. R. Granfors, B. A. Fraas, and R. O. Simmons, J. Low Temp. Phys. **67**, 353 (1987).
[9] I. Schuster, E. Polturak, Y. Swirsky, E. J. Schmidt, and S. G. Lipson, J. Low Temp. Phys. **103**, 159 (1991).
[10] A. R. Allen, M. G. Richards, and J. Schratter, J. Low Temp. Phys. **47**, 289 (1982).
[11] B. Chaudhuri, F. Pederiva, and G. V. Chester, J. Low Temp. Phys. **113**, 751 (1998).
[12] F. Pederiva, G. V. Chester, S. Fantoni, and L. Reatto, Phys. Rev. B **56**, 5909 (1997).
[13] T. McFarland, S. A. Vitiello, L. Reatto, G. V. Chester, and M. H. Kalos, Phys. Rev. B **50**, 13 577 (1994).
[14] R. A. Aziz, V. P. S. Nain, J. S. Carley, W. L. Taylor, and G. M. McConville, J. Chem. Phys. **70**, 4330 (1979).
[15] S. Moroni, D. E. Galli, S. Fantoni, and L. Reatto, Phys. Rev. B **58**, 909 (1998).
[16] R. A. Aziz, A. R. Jansen, and M. R. Moldover, Phys. Rev. Lett. **74**, 1586 (1998).